Biosensors and Bioelectronics 77 (2016) 315–322

Contents lists available at ScienceDirect

Biosensors and Bioelectronics

journal homepage: www.elsevier.com/locate/bios

Small biomolecule immunosensing with plasmonic optical fiber grating sensor

Clotilde Ribaut [a,b,*], Valérie Voisin [b], Viera Malachovská [a,b], Valentin Dubois [a], Patrice Mégret [b], Ruddy Wattiez [a], Christophe Caucheteur [b,**]

[a] Proteomics and Microbiology Laboratory, University of Mons, Mons, Belgium
[b] Electromagnetism and Telecommunication Department, University of Mons, Mons, Belgium

ARTICLE INFO

Article history:
Received 12 June 2015
Received in revised form
7 September 2015
Accepted 10 September 2015
Available online 12 September 2015

Keywords:
Fiber optic biosensor
Tilted fiber Bragg grating
Surface plasmon resonance
Cytokeratin 7 biomarker
Small biomolecule detection

ABSTRACT

This study reports on the development of a surface plasmon resonance (SPR) optical fiber biosensor based on tilted fiber Bragg grating technology for direct detection of small biomarkers of interest for lung cancer diagnosis. Since SPR principle relies on the refractive index modifications to sensitively detect mass changes at the gold coated surface, we have proposed here a comparative study in relation to the target size. Two cytokeratin 7 (CK7) samples with a molecular weight ranging from 78 kDa to 2.6 kDa, respectively CK7 full protein and CK7 peptide, have been used for label-free monitoring. This work has first consisted in the elaboration and the characterization of a robust and reproducible bioreceptor, based on antibody/antigen cross-linking. Immobilized antibodies were then utilized as binding agents to investigate the sensitivity of the biosensor towards the two CK7 antigens. Results have highlighted a very good sensitivity of the biosensor response for both samples diluted in phosphate buffer with a higher limit of detection for the larger CK7 full protein. The most groundbreaking nature of this study relies on the detection of small biomolecule CK7 peptides in buffer and in the presence of complex media such as serum, achieving a limit of detection of 0.4 nM.

1. Introduction

Biomarkers are becoming increasingly important for therapeutic decision, in particular, in the cancer diagnosis. Protein biomarkers appear to be excellent indicators since they are correlated to the presence of pathogenic processes and diseases. Furthermore, their detection remains the most specific and sensitive technique at early stage of cancer. Consequently, protein biomarkers detection is a promising tool for the first-phase tumor detection.

Numerous technologies are employed to identify biomarkers, including the genetic and proteomic analysis (Kisluk et al., 2014), the immunohistochemistry (Pohl et al., 2014) and the quantitative polymerase chain reaction "Q-PCR" (Inoue et al., 2012). Most of the patient materials for biomarkers detections are post-operative tissue samples. Biopsies are applied when a cancer is suspected and consequently are realized often at an advanced stage of the disease. Furthermore, surgeon interventions are invasive and cannot be used repeatedly.

Investigations of protein biomarkers can also be realized on biological fluids, such as blood, pleural effusion or urines (Silva et al., 2012; Kisluk et al., 2014). Fluids not only have a great advantage due to their accessibility but can reflect the pathological process as well. Blood sample's analysis, for example, is of great interest since tumors are known to release biomarkers into the bloodstream, circulating tumor cells and fragments of tumor-cell DNA. However, liquid samples present a relative stability since proteins are not stable in non-physiological conditions. Furthermore, they are complex samples that need to go through different purification steps before analysis.

Generally, the current diagnostic tools are time-consuming and are therefore not applicable for intraoperative diagnosis. The search of an appropriate technology platform in the aim to improve biomarkers detection for early diagnosis has led to a new rapid method based on a label-free detection of biomarkers thanks to biosensors. These analytical devices are made up of two parts: a bioreceptor that detects an analyte and a transducer that transforms the signal resulting from the biological interaction into a quantifiable signal (Perumal and Hasdhim, 2014). Recently, several biosensors such as electrochemical (Silva et al., 2014), piezoelectric (Arif et al., 2015; Uludag and Tothill, 2010) and optical probes (Mukundan et al. 2009) have been employed to detect biomarkers

* Corresponding author at: Proteomics and Microbiology Laboratory, University of Mons, Mons, Belgium.
** Corresponding author.
E-mail addresses: clotilde.ribaut@umons.ac.be (C. Ribaut), christophe.caucheteur@umons.ac.be (C. Caucheteur).

http://dx.doi.org/10.1016/j.bios.2015.09.019
0956-5663/

which offer a direct and quantitative detection of synthetic analytes.

In the literature, many works have been published on biosensors using surface plasmon resonance (SPR) as transducing mechanism (Homola, 2008; Patching, 2014; Velasco-Garcia, 2009). In fact, SPR sensing has been demonstrated to be an exceedingly powerful and quantitative probe for the interactions of a variety of biomolecular interactions, including protein/ligand. An important advantage of SPR is its high sensitivity without any labeling of the interactants, coupled with an acquisition of data extremely rapid. SPR based biosensors have been used to detect a large variety of analytes including cells, DNA and various cancer biomarkers (Altintas and Tothill, 2013), which correspond most often to large biomolecules. However, it is interesting to note that most of the SPR biosensors have been used to detect full proteins and very few for targeting small biomolecules. To explain the reasons, their operating principle consists in the excitation of a surface plasmon at the interface between a metal film and a dielectric medium. SPR sensor relies thus on the monitoring of refractive index changes at the surface of the sensor and is consequently mass dependent. Most of the SPR biosensors work according to the Kretschmann Prism compatible with flat surface (Gopinath, 2010).

More recently, a new promising class of SPR biosensors has emerged, the optical fiber (OF) biosensor (Espinosa Bosch et al., 2007; Velasco-Garcia, 2009). Fiber-optic SPR sensors present the highest degree of miniaturization compared to all other SPR sensors (Homola, 2008). Different configurations allow to excite surface plasmons at the nanometric metal coated surface of the OF when light is brought into contact with the surrounding medium (Caucheteur et al., 2015a, 2015b). The most often encountered fiber-optic sensors based on SPR are made of unclad fibers covered with a nanometric layer of gold (Pollet et al., 2009; Shrivastav et al., 2015). In addition, the fiber grating technology such as long period grating (LPG), or tilted fiber Bragg grating (TFBG) (Albert et al., 2012; Caucheteur et al., 2013, 2015b) also allows to excite SPR. To summarize, upon contact with the grating photo-inscribed inside the optical fiber, light confined in the core is outcoupled and consequently enters in contact with the nanometric metal layer, coated in the central region of the grating, creating excitation of the plasmon resonance. Our interrogation system made of TFBG, illustrated in Fig. 1A, has several unique advantages (Albert et al., 2012). First, measurements are realized at the near infrared wavelengths between 1500 and 1600 nm with a spectral width of the resonance between 0.01 and 0.1 nm, yielding a high Q-factor with unprecedented figure of merit. A high Q-factor is important since it arises both the sensitivity and the limit of detection of the sensor. It also ensures a full compatibility with the telecommunication-grade equipment. Second, with near infrared TFBGs we are able to compensate temperature fluctuations thanks to the presence of the core mode resonance in their amplitude spectrum, the so-called Bragg mode, as depicted in Fig. 2A. Last but not least, TFBGs allow a straightforward injection of polarized light, which is essential for proper SPR generation, as it will be highlighted in the following.

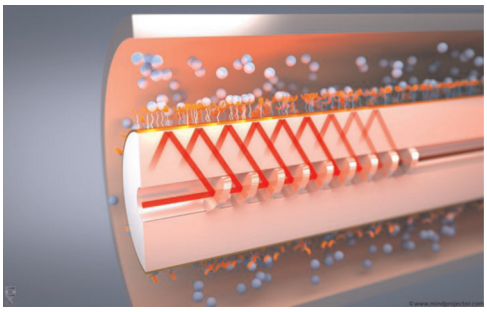

Fig. 1. Principle of the experimental set-up with a scheme of the optical fiber made of a cladding covered with antibodies immobilized on a nanometric layer of gold, and a core with tilted fiber Bragg grating inscribed in.

Gold-coated optical fiber biosensors, based on TFBG technology, have been already reported and the most crucial aim is attaining non-invasive and effective diagnosis (Albert et al., 2013; Guo et al., 2014; Shevchenko et al., 2011; Voisin et al., 2014; Malachovska et al., 2015). In fact, the micrometer size of the optical fiber biosensor offers new horizon, notably in biomedical applications such as introduction into a catheter, which can be of interest for early cancer diagnosis. Once again, optical fiber biosensors have been tested in the presence of large proteins. In view of the good sensitivity of this technology, we propose here to test with small biomolecules. To do so, we have focused our study on the lung cancer diagnosis.

A diverse range of tumor markers has been associated with lung cancer (Altintas and Tothill 2013; Flores-Fernandez et al., 2012). In this study, we focused on cytokeratins 7 (CK7). In fact cytokeratins are particularly useful tools for diagnosis in oncology (Sawant et al., 2008). In particular, CK7 profile of lung tumor has proved to be a useful aid in the differential diagnosis of carcinomas, since primary and metastatic tumors present different profiles. In fact, primary lung tumors express cytokeratin 7 (CK7+) while secondary tumors are deficient in CK7 (CK7−) (Campbell and Herrington, 2001). Moreover, it has been demonstrated that cytokeratin fragments can be released from malignant cells and consequently CK fragments can be located in blood circulation (Man et al., 2014) and are therefore easily accessible with an optical fiber properly modified.

In order to selectively detect cytokeratin 7 target with the SPR-TFBG, the gold coated optical fiber has to be functionalized. The development of a bioreceptor remains a crucial step, since stability and hardiness of bioreceptor immobilization onto optical fiber govern the biosensor performance. In fact, the recognition element immobilization rules specificity, selectivity, sensibility and reliability of the biosensor response. Among the several molecular edifices to detect cytokeratin proteins, our choice is focused on the commonly used antibody/antigen cross linking thanks to a first self-assembled monolayer (SAM) of thiols immobilized onto gold. SAMs are well-defined and described in the literature (Ulman, 1996; Love et al., 2005). SAMs are highly ordered and oriented and have the advantage to incorporate a wide range of groups both in alkyl chain and at the chain terminal, especially carboxylate function used to covalently immobilize antibodies thanks to a peptide bond. Furthermore, the biocompatible nature of SAMs makes them excellent structures for biomedical applications.

The cytokeratin 7 antigen detection by the bioreceptor is based on the specific chemical reaction with its corresponding antibody (AbCK7). The operating principle is based on the recognition of the cytokeratin 7 antigen epitope by the fragment antigen-binding (Fab), a region present on the cytokeratin 7 antibody. In addition to the full protein detection made of 469 amino acids, corresponding to a large biomolecule, we propose here to monitor a protein fragment called cytokeratin 7 peptide (CK7pep) made of only 23 amino acids in order to present a comparative study depending on the size of the target. In fact, the detection of small molecule antigens remains a challenge in the SPR immunosensing. Most of the SPR biosensors are based on large molecule detection since SPR response in presence of small mass suffers from various disadvantages not encountered with full protein, such as low signal-to-noise ratio. Nevertheless, new studies have proposed to offer small molecule SPR fiber-optic biosensors as proposed by Singh et al. with the detection of phenolic compounds (Singh et al., 2013). Our work features the first experimental evidence about reliable detection of small proteins with near-infrared plasmonic optical fiber biosensors. In addition to the small biomolecules

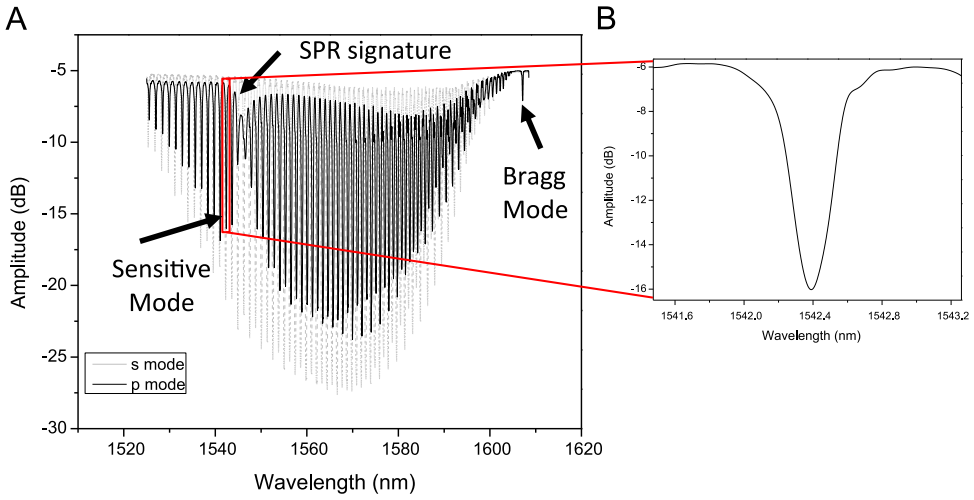

Fig. 2. (A) Full transmitted SPR-TFBG signal response in s (azimuthal) and p (radial) polarized light composed with numerous modes and (B) a zoom on the most sensitive mode, core of our detection system.

detection challenge, the developed biosensors were tested in the presence of a complex buffer mimicking physiological conditions, further attesting their robustness.

2. Materials and methods

2.1. Chemicals

Fetal bovine serum (FBS); Tween 20; N-Hydroxysuccinimide (NHS); N-(3-Dimethylaminopropyl)-N′-ethylcarbodiimide hydrochloride (EDC), Tween 20, Tetramethylbenzidine (TMB) and phosphate buffer saline (PBS) were purchased from Sigma-Aldrich. Tris were furnished by Merck. The nitrocellulose membrane comes from GE Healhtcare Life sciences, and ECL reagent from Promega. Cytokeratin 7 antibodies (AbCK7) and cytokeratin 7 peptide (CK7) were from Biorbyt. The cytokeratin full protein (CK7FP) was purchased from abcam. Bovine serum albumin (BSA) was form Acros. The dithiolalkanearomaticPEG6-COOH (S_2PEGCOOH) came from SensoPath technology. Buffers were prepared in milliQ water.

2.2. Biosensor preparation

2.2.1. Fabrication of TFBGs

A ca. 50 cm long portion of a telecommunication grade single-mode optical fiber (Corning SMF-28, 125 μm uncoated silica fiber diameter) was used to prepare each sensor. TFBGs were inscribed in the fiber core with external tilt angles varying between 7° and 9°. 1 cm long TFBGs were photo-inscribed using a frequency-doubled argon-ion laser emitting at 244 nm and a 1090 nm period phase mask tilted in the plane perpendicular to the incident beam, as described in our previous work (Caucheteur and Mégret, 2005).

2.2.2. Gold coating deposition and thermal annealing

The uncoated silica fibers at the TFBG location were coated with a nanometric gold film. The standard sputtering process was realized by high vacuum sputter coater (benchtop Leica EM SCD500) and gold (Au, 99.99% purity) sputtering target. Approximately 50 nm of gold were deposited in air at room temperature by a double deposition with a fiber rotation. Gold film thickness was controlled and monitored in real-time by a build-in quartz micro-balance (Leica EM QSG100).

Freshly deposited gold films around TFBGs were thermally annealed at 200 °C for 1 h in order to improve gold attachment on silica. The system consists of an enclosed Switching Power Supply (25 W, 5 V, 5 A) and a hand-crafted helical coil to heat a longitudinal section of the optical fiber containing the TFBG.

2.2.3. Bioreceptor development

The optical fiber gold sensitive area was functionalized according to a four steps protocol. To start, gold was cleaned with ethanol by immersion for 2 h at room temperature and dried under nitrogen. Then, the gold area was immersed in a solution of S_2PEGCOOH at 2 mM in ETOH overnight at room temperature to form an ordered self-assembled monolayer. Optical fiber was then rinsed with ETOH and dried under nitrogen. Esterification reaction of carboxylate functions was realized by an immersion of the OF in a mixture of NHS/EDC (1:5 M/M) in H_2O milliQ for 2 h at room temperature. The surface was then rinsed with milliQ water and dried under nitrogen. The sensitive area was immediately immersed in AbCK7 solution, at 20 μg/mL in PBS 10 mM at pH 7.4, for 2 h at room temperature. Again, the surface was rinsed with PBS. The blocking step was realized by immersion of the optical fiber in BSA solution 1% (w/v) in PBS for 1 h. Bioreceptor was finally rinsed with PBS and stored in a petri dish. Cytokeratin 7 antibodies conjugated with fluorescein isothiocyanate (FITC) fluorophore were used for confocal fluorescence experiments instead of AbCK7.

2.3. Surface characterization

2.3.1. Atomic force microscopy

The nanoscale investigation of the optical fiber surface was carried out by Atomic Force Microscopy (AFM) using ICON instrument (from Bruker Corporation, Santa Barbara, CA, USA) by Peak Force quantitative nanomechanical mapping (QNM) in air mode, at room temperature, with a silicon-tip on nitride lever (SNL from Brucker). AFM images were recorded at each step of the bioreceptor elaboration on several locations on the top of the optical fiber, with scan area of $1 \times 1\ \mu m^2$. AFM images were analyzed using the Nanoscope image analysis program. The root mean square (RMS) value represents the standard deviation of the height images.

2.3.2. Confocal microscopy

Fluorescence images were recorded using FluorView Laser Scanning Confocal microscope (FV1000, Olympus) and software. Optical fiber samples were fixed on glass slides and observed at $\times 20$ magnification with a fluorescein isothiocyanate (FITC) filter. Imaris software was used to treat 3D images.

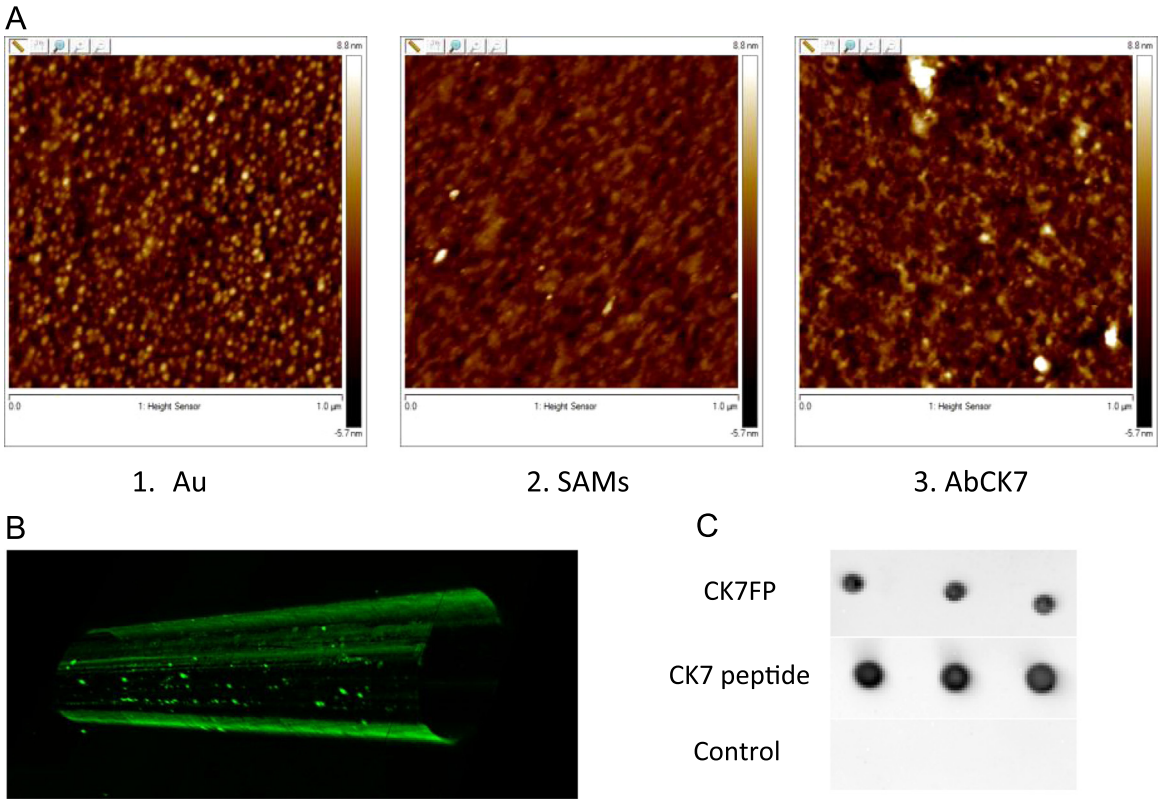

Fig. 3. (A) AFM height images on optical fiber at each step of the bioreceptor elaboration, starting with: (A.1) Au layer; follow by (A.2) SAM; then by (A.3) antibodies immobilization. (B) Confocal microscopy 3D image of the optical fiber functionalized with SAM in presence of antibodies conjugated with FITC fluorophore. (C) Dot Blot performed using cytokeratin 7 antibodies for detection of cytokeratin full protein (CK7FP), cytokeratin 7 peptide, and a negative control.

2.4. Antigen/antibody affinity

2.4.1. Dot blot

0.1 μg of cytokeratin 7 samples (peptide and full protein) were spotted onto nitrocellulose membrane, dried under air, and blocked in 3% (*w*/*v*) BSA in TBS-T (0.05% Tween 20 in TBS) mixture overnight at room temperature. The membrane was then immersed in primary antibody (AbCK7) at 1:500 dilution in 0.1% (*w*/*v*) BSA/TBS-T for 30 min at room temperature. After three washing with TBS-T, the membrane was incubated with the secondary antibody conjugated with horseradish peroxidase at 1:5000 dilution in 0.1% BSA/TBS-T for 30 min at room temperature. The membrane was then washed twice 5 min in TBS-T, then once in TBS. Finally, the membrane was incubated with ECL reagent for 1 min before exposure to chemiluminescence.

2.4.2. Elisa

The K_d values were determined as previously described by Kim et al. (1990). Briefly, cytokeratin 7 antigens (CK7 peptide or full protein) at various concentrations were mixed with a constant amount of CK7 antibody. After an overnight incubation at 4 °C, 200 μL of each mixture were transferred into wells previously coated with antigens and incubated for 1 h00 at 37 °C. The mixture was then incubated in presence of tetramethylbenzidine (TMB) for 0.5 h, and finally H_2SO_4 was added to stop the reaction. Then absorbance at 450 nm was measured using a plate analyzer (FluoStar Optima, BMG Labtech). The average K_d is obtained by plotting the experimental data as $A_0/(A_0-A)$ versus $1/Ag_0$, where the slope is equal to K_d. A_0 is the absorbance of antibodies measured in solution by ELISA in the absence of antigens; A is the absorbance in presence of antigens and Ag_0 is the initial concentration of antigen in solution.

2.5. SPR detection system

2.5.1. Experimental set-up

Gold-coated optical fiber biosensors are connected to optical vector analyzer (OVA) from LUNA technology for transmission measurements according to our previous work (Voisin et al., 2014). Typical transmission spectra obtained with a TFBG immersed in aqueous solution present comb-like cladding modes resonances featuring an SPR signature and a Bragg mode, as shown in Fig. 2A. The analysis of the data presented in this paper is based on the monitoring of the most sensitive mode. According to previous studies, the SPR portion remains the zone of interest. In fact, it was demonstrated that the mode situated on the shoulder of the SPR envelope (so-called +2 mode) in our former work (Caucheteur et al., 2015), corresponds to the most sensitive mode of the TFBG transmitted spectrum. Consequently, analyses of the data on this paper are focused on the amplitude evolution of the mode +2 during detection of antigens. Results are presented as the biosensor response as a function of CK7 concentration, with two thresholds. One corresponds to the reference signal measured in the absence of antigen while the second threshold matches with the maximum expressing the saturation of the antibodies by its specific antigens.

3. Results and discussion

3.1. Bioreceptor development

The first step of the elaboration of the gold coated SPR-TFBG biosensor remains the bioreceptor's functionalization. This step remains crucial since the biosensor performance rests on its robustness. The molecular edifice manufacturing has thus required a

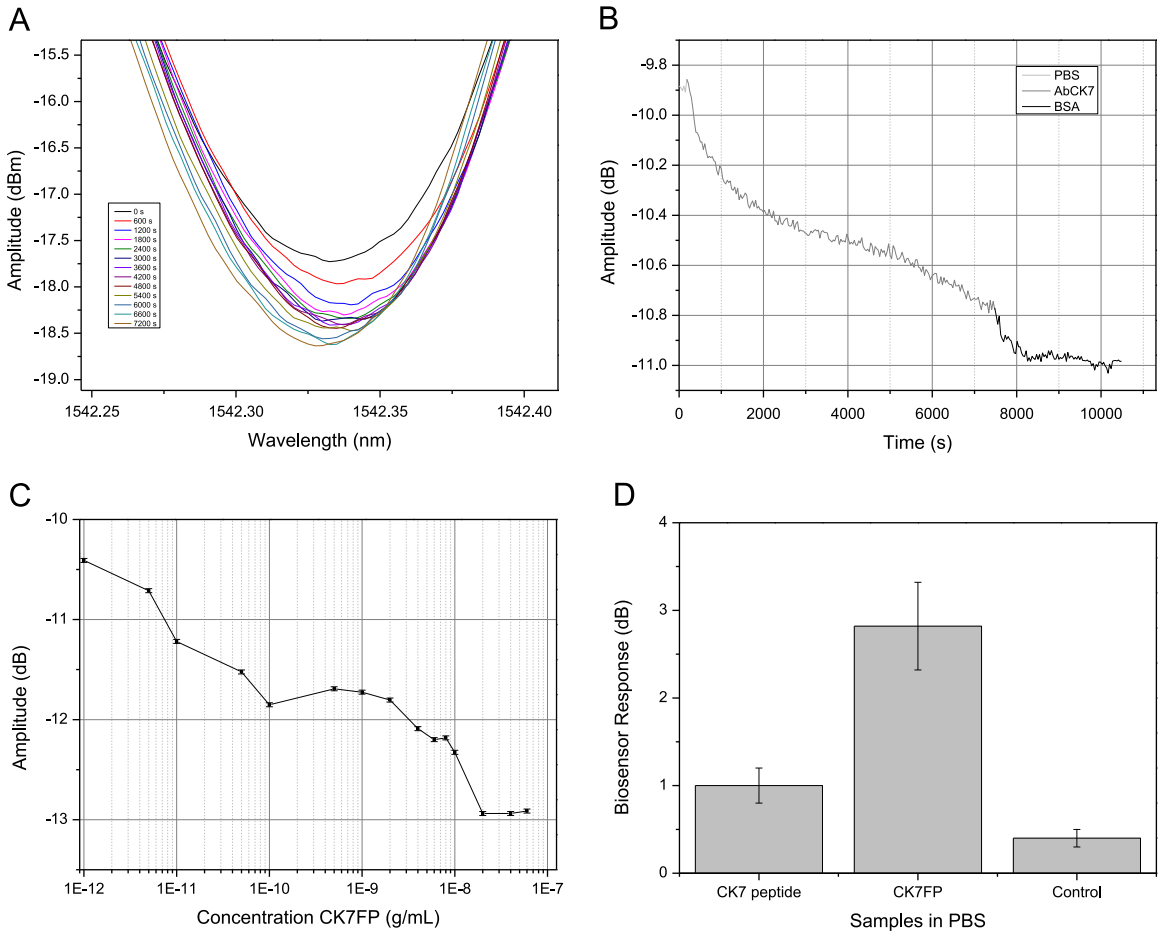

Fig. 4. (A) Shift of the sensitive mode during immobilization of antibodies on the optical fiber pretreated with SAM. (B) Amplitude monitoring of the sensitive mode during AbCK7 incubation follow by the blocking step by BSA treatment. (C) Amplitude monitoring of the sensitive mode in presence of CK7FP at different concentrations diluted in PBS. (D) Biosensor response obtained for optical fiber functionalized with AbCK7, in presence of CK7 peptide or CK7FP in comparison with OF functionalized without AbCK7.

surface characterization study, in order to optimize the immobilization of antibodies on the optical fiber surface.

A TAG made of a disulfide self-assembled monolayer coupled with six Polyethylene Glycol (PEG) groups and finally the carboxylate terminal function was used as functionalized layer. The cytokeratin antibodies (AbCK7) immobilization on SAMs requires an esterification reaction of the carboxylate by a couple NHS/EDC, in order to form a peptide bond between the terminal ester of SAMs and the numerous amines present on antibodies.

The surface characterization of the bioreceptor, during the different functionalization steps, has been carried out by Atomic Force Microscopy (AFM) and confocal fluorescence, two techniques that have enabled the surface analysis of the optical fiber surface, directly. AFM analysis has been first realized on optical fiber covered with approximately 50 nm of Au sputtered before and after deposition of thiol compounds. The regular dots characteristics of gold layer (Fig. 3A) have been masked by the thin organic self-assembled layer made of thiols (Fig. 3A). Root mean square (RMS) roughness values, calculated from the software nanoscope analysis, have confirmed the evolution of the surface during the bioreceptor elaboration. RMS value decreases after thiol deposition ($RMS_{Au} = 1.9$ nm $> RMS_{SAM} = 1.1$ nm) since SAM forms a compact monolayer of 2 nm, which flattens the surface.

Secondly, AFM measurements have been performed after the immobilization of antibodies on the SAM. Fig. 3A reveals new dots (white spots, protrusions of the height images) due to the presence of large molecules attributed to antibodies AbCK7. In fact, the size of the aggregate estimated at 15 nm corresponds to the dimensions of the antibody. Furthermore, the presence of larger molecules such as proteins on the surface increases the roughness of the surface ($RMS_{AbCK7} = 2.00$ nm). These results have put in evidence the topological surface modification at each step of the bioreceptor elaboration, which is a sign of the presence of cytokeratin 7 antibodies presence on the surface.

Since the manipulation of antibodies is delicate and depends on the protein's nature, AbCK7 immobilization has required protocol modifications in order to reach the most homogeneous layer. Consequently, covalent links between antibodies and NHS terminal function of the SAM activated have been investigated. Changes of pH, temperature, incubation time and concentrations during immersion of the optical fiber, have been performed and controlled by confocal microscopy. Fig. 3B shows an optical fiber functionalized with cytokeratin 7 antibodies conjugated with FITC fluorophore. Even though the optical fiber surface is not entirely covered, the 3D image of the OF presents a good fluorescent distribution around the optical fiber. This result is in good agreement with AFM analysis concerning the effective functionalization of the optical fiber surface.

3.2. Cytokeratin 7 targets/cytokeratin 7 antibodies recognition

Since the biosensor concept is based on the antibody/antigen affinity, an analysis has been performed in order to guarantee the affinity between cytokeratin antibodies and the two cytokeratin 7 samples (CK7FP and CK7pep) separately. A technique for detecting both CK7 by using Dot Blot method has clearly highlighted

the signal of the antibody/antigen interaction, confirming the affinity between AbCK7 and both samples. Fig. 3C presents the characteristic dark spot (triplicate) revealed by chemiluminescence for both CK7 samples while no signal was detected for a negative control.

3.3. SPR-TFBG monitoring on a simple buffer

3.3.1. In situ monitoring of cytokeratin 7 antibodies In phosphate buffer

For the experimental set-up, SPR-TFBG was firstly used on the AbCK7 immobilization's onto optical fiber surface. SPR-TFBG spectra were recorded *in situ* every 30 s thanks to a LabVIEW software. Data were then processed by a Matlab program and presented as the monitoring of the amplitude of the most sensitive mode as a function of time (Fig. 4B). Fig. 4A represents the overlapping of the mode of interest, recorded every 10 min over a period of 2 h. The monitoring of the sensitive mode of SPR-TFBG response during AbCK7 incubation time of an optical fiber, pretreated with SAM and NHS/EDC, clearly shows an evolution of the amplitude (-0.9 dB) attributed to the immobilization of AbCK7 on the OF surface (Fig. 4B). This experiment has also demonstrated the last step of the bioreceptor elaboration. SPR-TFBG has, in fact, monitored the blocking treatment, performed to avoid non-specific interactions, realized with the BSA protein. In addition to confirm the bioreceptor manufacturing, this SPR monitoring put in evidence the time required for antibodies' immobilization. Fig. 4B shows a fast decrease of the amplitude for 30 min, the time required to establish the peptide bond.

3.3.2. In situ monitoring of cytokeratin7 full protein detection in phosphate buffer

Once the optical fiber has been functionalized with cytokeratin 7 antibodies, it was immersed in corresponding cytokeratin 7 full protein (CK7FP) solutions for monitoring by the interrogation system. To reach the sensitivity of the biosensor, initial measurements were realized in a phosphate buffer (PBS) with increasing CK7FP concentrations from 1E-12 g/mL to 1E-6 g/mL. Recording of the transmission spectrum during experiments put in evidence an evolution of the SPR-TFBG response during the first seconds. In fact, in a first phase, a shift of the amplitude signal was observed as soon as antigens have been injected proving the high affinity between the target and its corresponding antibody. Then in a second phase, the amplitude evolved until the signal had stabilized. This evolution can be explained by the reversibility of the antibody/antigen reaction. For all experiments, SPR-TFBG spectra were recorded after stabilization of the signal. Fig. 4C corresponds to the data recorded for a functionalized fiber, representing the usual amplitude evolution of the sensitive mode depending on Log 10 CK7FP concentrations.

As illustrated in Fig. 4C, decrease in amplitude of the sensitive mode was observed starting from 3E-12 g/mL until it has reached a threshold at 2E-8 g/mL. Amplitude monitoring can be decomposed into three parts; a first phase with a high-amplitude shift until 1E-10 g/mL due to the large number of antibodies accessible on the surface. A second phase with a smaller shift of the amplitude between different CK7FP injections was then noticed from 1E-10 to 2E-8 g/mL. This reduction in amplitude shift can be explained by the significant decline of available antibodies. Finally, the third and last step was observed at 2E-8 g/mL by a minimal threshold assigned to the saturation of AbCK7 on the sensor surface.

The experiment was repeated on three distinct fibers, engineered in the exact same conditions, starting from the inscribed angle of the grating, to the bioreceptor functionalization protocol. Results were determined by calculating the total shift reached between the maximal amplitude and the minimal threshold. The statistical analysis of the triplicate resulted in an average amplitude shift of $2.8+/-0.5$ dB (Fig. 4D) for the cytokeratin 7 full protein detection in a phosphate buffer. Furthermore, it is interesting to note that CK7FP was detected from 3E-12 g/mL in PBS. Such observations indicate that the biosensor was highly responsive since our sensitivity, estimated lower than 1 pM, is very good. In our work, it is important to note that the sensitivity was reached for a full protein with a molecular weight of 78 kDa and an affinity with its corresponding antibody characterized by a dissociation constant $Kd = 6.8 \times 10^{-9}$M.

Henceforth, as in most of SPR biosensors, detections focused on targeting full proteins, corresponding to large biomolecules. Given the sensitivity of our device, we propose here to detect smaller target using the same approach, based on antibody/antigen. We have thus tested the SPR-TFBG on a fragment of the cytokeratin 7 peptide, made of 23 amino acids (SRAEAEAWYQTKFETLQAQAGKH), with a molecular weight of 2.6 kDa. This experiment was realized in the aim to highlight the sensor performance in the presence of a small target.

3.3.3. In situ monitoring of cytokeratin 7 peptide detection in phosphate buffer

Using the same functionalization protocol on the gold coated TFBG, cytokeratin 7 peptide (CK7pep) has been injected. Once again, three distinct TFBGs, prepared under similar conditions, were used for CK7 peptide detection in a phosphate buffer, in order to perform statistical analysis on triplicates. As previously, SPR-TFBG response has been registered during injection of CK7 peptide at different concentrations diluted in a phosphate buffer. Interestingly, the trend is similar to the one presented in Fig. 4C. Nevertheless, differences between CK7pep and CK7FP detection have been noticed during experiment. Firstly, amplitude shift has been measured from 1E-9 g/mL instead of 2E-12 g/mL, secondly the final amplitude measured between the maximal and the minimal threshold has been determined at $1.0+/-0.2$ dB against 2.8 dB for CK7FP, as illustrated in Fig. 4D.

First measurements in a phosphate buffer have put in evidence the sensitivity of the biosensor towards cytokeratin samples. It is interesting to note that the refractive index (RI) has never progressed during all experiments, regardless of the sample's nature (CK7FP and CK7pep) and the concentration. The value was equal to the phosphate buffer RI value ($RI_{PBS} = 1.3350$ RIU) all along. Therefore, amplitude shifts observed during successive injections were due to biomolecules attachment on the surface and not due to the surrounding media. Logically, we can note that the variation of the amplitude resonance between the couple AbCK7/CK7pep has been less intense than the ones observed in presence of the full protein. Furthermore, a decrease of the sensitivity was determined for the peptide in comparison with the full protein. These results are in good accordance with our expectations, since the biosensor device depends on the refractive index changes at the penetration depth of the sensing field. The cytokeratin 7 full protein, made of 469 amino acids, as being larger than CK7 peptide, has logically been detected with a higher sensitivity. However, mass does not remain the only parameter to take into account for SPR detection. In fact, biosensor sensitivity depends also on the affinity between the couple antibody/antigen, characterized by the dissociation constant Kd.

Consequently, we have determined the affinity of the CK7 antibody towards the two antigens by calculating the average Kd of AbCK7/CK7pep and AbCK7/CK7FP, by use of ELISA technique. Experiments have revealed a Kd equal to 8E-10 M for AbCK7/CK7 peptide against 6E-9 M for the full protein. As a consequence, these experimental Kd have put in evidence a better affinity for the peptide. Results were logic since the peptide sequence was

used as immunogen for the polyclonal antibodies production. Nevertheless, ELISA tests have demonstrated a correct affinity between AbCK7 and the full protein. The highest CK7FP Kd can be explained by the lower accessibility of the epitopes in the full protein conformation, in comparison with a probable linear shape of the peptide. Consequently, it is interesting to note that in spite of a lower affinity towards antibodies, SPR experiments have clearly put in evidence a better limit of detection for the CK7 full protein, proving that this technique is largely mass dependent.

In addition to the Kd determination, ELISA measured data allowed also to confirm the measured signal of the biosensor. In fact, recording of the optical density (OD) with increasing AbCK7 concentration have highlighted a similar trend to the Fig. 4C, with an increase of OD until the signal reached a threshold (Supplementary data).

Finally, to ensure that the biosensor response is not due to non-specific attachments on the surface, a control measurement has been conducted. In the functionalization protocol, the bioreceptor has been treated with a commonly used blocking agent (BSA) in order to avoid non-specific interactions. Experiments with CK7 target realized on optical fiber functionalized with SAM and BSA but in the absence of antibodies (AbCK7) on the surface have demonstrated the effectiveness of the blocking step since no significant evolution of the amplitude was observed (Fig. 4D). As with other experiments, performed in non-complex buffer, error's bars represent the variation measured for three samples prepared in the same conditions.

Experiments conducted in a phosphate buffer have successfully demonstrated a good sensitivity for the detection of cytokeratin 7 antigens. This study has revealed once again the very good sensitivity towards full protein, but the most interesting part has remained in the small biomolecules detection. Furthermore, triplicates confirm the good reproducibility of the technique. In fact, it could be a very promising tool to detect small biomolecule, especially peptides, in fluid sample. Since the concept of the biosensor relies on medical diagnosis, following experiments have consisted in the peptide detection on complex media mimicking physiological conditions. In this context, next experiments of the gold coated optical fiber biosensor were performed on phosphate buffer complemented with 10% fetal bovine serum (FBS), resulting on a complex buffer full of proteins including albumin, enzymes and others; as well as vitamins and nutrients. Objectives were to get close to physiological conditions on the one hand, and to guarantee the selectivity of the biosensor on the other hand. In the presence of FBS in the media, the optical fiber ended up with numerous compounds able to attach on the surface. In fact, all proteins are made of amino acids composed of amine functions that have a good affinity with gold surface. In consequence, bioreceptor preparation gains in importance to ensure the selectivity of the SPR response.

3.4. *In situ monitoring of CK7 peptide in a complex solution*

The study on complex media has started on three independent optical fibers functionalized with AbCK7 and immersed in PBS supplemented with 10% (v/v) FBS for several minutes in the absence of cytokeratin 7 peptide. First, we can note a change of the refractive index of the surrounding media (RI) in comparison with

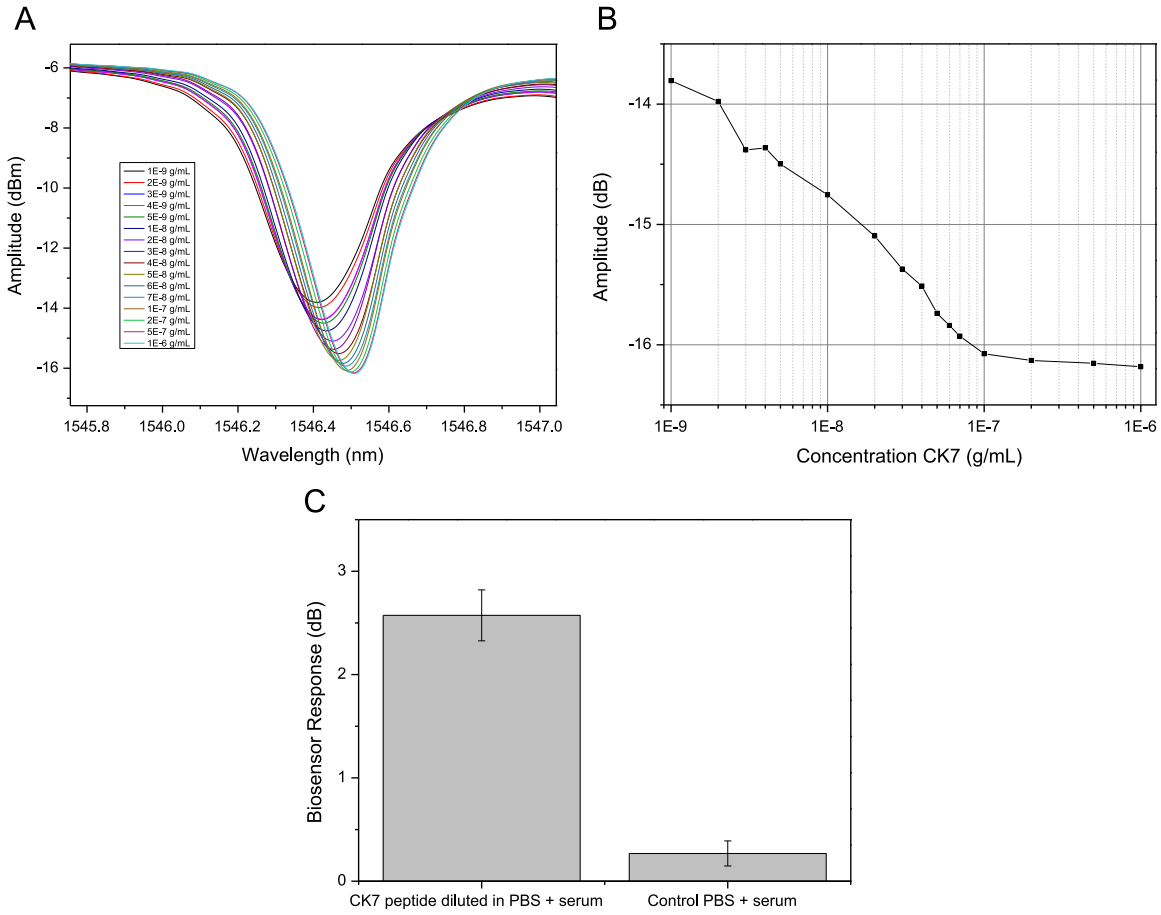

Fig. 5. (A) Shift of the sensitive mode during incubation of the optical fiber functionalized with AbCK7 on CK7 peptide at different concentrations diluted in PBS+10% FBS. (B) Amplitude monitoring of the sensitive mode during CK7 peptide incubation. (C) Biosensor response obtained for optical fiber functionalized with AbCK7 immersed in PBS+10% FBS, in presence or in absence of CK7 peptide.

phosphate buffer (RI_{PBS} = 1.3349 RIU *vs* RI_{FBS} = 1.3357 RIU). The 0.0008 RIU difference creates a shift of 1.5 nm in wavelength. Secondly, stability of the SPR-TFBG signal notably in amplitude for half an hour has demonstrated that the blockage step was efficient since no interaction takes place between numerous proteins present in the media and the OF surface (Fig. 5C). The amplitude shift evolution has been observed starting form injection of the target CK7 antigen in the surrounding media. Experiments with a functionalized optical fiber were repeated as previously with increasing CK7 concentration from 1E-9 g/mL to 1E-6 g/mL diluted in PBS containing 10% (v/v) FBS. As with previous tests in PBS, the amplitude shift was observed immediately. Then its stabilization has required few seconds. SPR-TFBG spectra have been recorded, for all experiments, after a stable baseline has been obtained.

The illustrated Fig. 5A reveals the evolution of the most sensitive mode during injection of CK7pep which highlights the detection of the target. The amplitude monitoring, as presented in Fig. 5B, clearly shows the evolution of SPR-TFBG signal as soon as the CK7pep was injected until it has reached a minimum threshold at 1E-7 g/mL. Fig. 5C presents the average output and errors for a three-fold repeated CK7pep detection on distinct optical fibers prepared on the exact same conditions. All three fibers have presented the identical amplitude evolution depending on the CK7 concentration, including an amplitude shift from 1E-9 g/mL, which identifies that the lowest concentration detected is estimated at 0.4 nM.

4. Conclusion

Results presented here are very promising for the lab-on-fiber concept since they demonstrate the ability of SPR-TFBG to detect cytokeratin 7 proteins, biomarkers of interest in the lung cancer diagnosis. The most crucial point concerns the detection of CK7 peptide, made of 23 amino acids with a corresponding molecular weight of 2.6 kDa. In comparison with the literature, CK7pep represents a small biomolecule of the size of few nanometers, which is still a big challenge in the biosensor field. Here, by monitoring the amplitude shift of the most sensitive mode of the SPR-TFBG spectra, the proposed biosensor was able to detect biomolecule interaction with the fiber surface, since the refractive index of the surrounding media did not evolve during experiments. Furthermore, optical fiber biosensors proposed here have highlighted the selectivity of the bioreceptor since this work has shown the ability to detect small targets from complex environment mimicking physiological conditions. SPR-TFBG biosensors combine the advantages of the small size of optical fiber with the low limit of detection of SPR sensors and with a rapid acquisition of data. For further insight into the biomarkers detection, our aim now is to improve the limit of detection by combining with the micro-fluidic technology while enhancing the antibody/antigen crosslinking that rules the biosensor efficiency.

Acknowledgments

The authors thank the laboratory for Chemistry of Novel Materials of the University of Mons for the access to AFM equipment and the valuable advices provided by Dr. Philippe Leclère and Dr. Mathieu Surin. This work is supported by the European Research Council (ERC) through the starting Independent Researcher Grant PROSPER (Grant Agreement no. 280161–https://www.umons.ac.be/erc-prosper), and by the F.R.S.-FNRS (Associate Researcher grant of C. Caucheteur).

Appendix A. Supplementary material

Supplementary data associated with this article can be found in the online version at http://dx.doi.org/10.1016/j.bios.2015.09.019.

References

Albert, J., Shao, L.-Y., Caucheteur, C., 2012. Laser Photonics Rev., 1–26.
Albert, J., Lepinay, S., Caucheteur, C., DeRosa, M.C., 2013. Methods 63, 239–254.
Altintas, Z., Tothill, I., 2013. Sens. Actuators B 188, 988–998.
Arif, S., Qudsia, S., Urooj, S., Chaudry, N., Arshad, A., Andleeb, S., 2015. Biosens. Bioelectron. 65, 62–70.
Campbell, F., Herrington, C.S., 2001. Curr. Diagn. Pathol. 7, 113–122.
Caucheteur, C., Mégret, P., 2005. Photonics Technol. Lett. IEEE 17, 2703–2705.
Caucheteur, C., Voisin, V., Albert, J., 2013. Opt. Express 21, 3055–3066.
Caucheteur, C., Guo, T., Albert, J., 2015a. Anal. Bioanal. Chem. 407, 3883–3897.
Caucheteur, C., Voisin, V., Albert, J., 2015b. Opt. Express 23, 2918–2932.
Espinosa Bosch, M., Ruiz Sanchez, A.J., Sanchez Rojas, F., Bosch ojeda, C., 2007. Sensors 7, 797–859.
Flores-Fernandez, J.M., Herrera-Lpoez, J., Sanchez-Llamas, F., Rojas-Calvillo, A., Cabrera-Galeana, P.A., Leal-Pacheeco, G., Gonzales-Palomar, M.G., Femat, R., Martinez-Velazquez, M., 2012. Expert. Syst. Appl. 39, 10851–10856.
Gopinath, S.C.B., 2010. Sens. Actuators B. 150, 722–733.
Guo, T., Liu, F., Liu, Y., Chen, N.-K., Guan, B., Albert, J., 2014. Biosens. Bioelectron. 55, 452–458.
Homola, J., 2008. Chem.Rev. 108, 462–493.
Inoue, M., hiyama, K., Nakabayyashi, K., Morii, E., Minami, M., Sawabata, N., shintani, Y., Nakagiri, T., Susaki, Y., Maeda, J., Higashiyama, M., Okami, J., Yoshida, Y., Ding, J., Otomo, Y., Okumura, M., 2012. Lung Cancer 78, 212–218.
Kim, B.B., Dikova, E.B., Sheller, U., Dikov, M.M., Gavrilova, E.M., Egorov, A.M., 1990. J. Immunol. Methods 131, 213–222.
Kisluk, J., Ciborowski, M., Niemira, M., Kretowski, A., Noklinski, J., 2014. J. Pharm. Biomed. Anal. 101, 40–49.
Love, L.C., Estroff, L.A., Kriebel, J.K., Nuzzo, R.G., Whitesides, G.W., 2005. Chem. Rev. 105, 1103–1169.
Malachovska, V., Ribaut, C., Voisin, V., Surin, M., Leclère, P., Wattiez, R., Caucheteur, C., 2015. Anal. Chem. 87, 5957–5965.
Man, Y., Cao, J., Jin, S., Xu, G., Pan, B., Shang, L., Che, D., Yu, Q., Yu, Y., 2014. J. Exp. Med. 234, 29–40.
Mukundan, H., Kubicek, J.Z., Holt, A., Shively, J.E., Martinez, J.S., Grace, K., Grace, W. K., Swanson, B.I., 2009. Sens. Actuators B 138, 453–460.
Patching, S.G., 2014. Biochim. Biophys. Acta. 1838, 43–55.
Perumal, V., Hasdhim, U., 2014. J. Appl. Biomed. 12, 1–15.
Pohl, M., Olsen, K.E., Holst, R., Ditzel, H.J., Hansen, O., 2014. Clin. Lung Cancer 15, 222–230.
Pollet, J., Delport, F., Janssen, K.P.F., Jans, K., Maes, G., Pfeiffer, H., Wevers, M., Lammertyn, J., 2009. Biosens. Bioelectron. 25, 864–869.
Sawant, S.S., Zingde, S.M., Vaidya, M.M., 2008. Oral Oncol. 44, 722–732.
Shevchenko, Y., Francis., T.J., Blair, D.A.D., Walsh, R., deRosa, M.C., Albert, J., 2011. Anal. Chem. 83, 7027–7034.
Shrivastav, A.M., Mishra, S.K., Gupta, B.D., 2015. Sens. Actuators B 212, 404–410.
Silva, C.L., Passos, M., Câmara, J.S., 2012. Talanta 89, 360–368.
Silva, M.L.S., Gutiérrez, E., Rodriguez, J.A., Gomes, C., David, L., 2014. Biosens. Bioelectron. 57, 254–261.
Singh, S., Mishra, K., Gupta, B.D., 2013. Sens. Actuators B 186, 388–395.
Uludag, Y., Tothill, I.E., 2010. Talanta 82, 277–282.
Ulman, A., 1996. Chem. Rev. 96, 1533–1554.
Velasco-Garcia, M.N., 2009. Semin. Cell. Dev. Biol. 20, 27–33.
Voisin, V., Pilate, J., Damman, P., Mégret, P., Caucheteur, C., 2014. Biosens. Bioelectron. 51, 249–254.